



A compact dual-band dual-port diversity antenna for LTE

Lila Mouffok, Anne Claire Lepage, Julien Sarrazin, Xavier Begaud

► To cite this version:

Lila Mouffok, Anne Claire Lepage, Julien Sarrazin, Xavier Begaud. A compact dual-band dual-port diversity antenna for LTE. *Advanced Electromagnetics*, 2012, [http://dx.doi.org/10.7716/aem.v1i1.42](http://dx.doi.org/10.7716/aem.v1i1.42.10.7716/aem.v1i1.42). hal-00983472

HAL Id: hal-00983472

<https://hal.science/hal-00983472>

Submitted on 25 Apr 2014

HAL is a multi-disciplinary open access archive for the deposit and dissemination of scientific research documents, whether they are published or not. The documents may come from teaching and research institutions in France or abroad, or from public or private research centers.

L'archive ouverte pluridisciplinaire **HAL**, est destinée au dépôt et à la diffusion de documents scientifiques de niveau recherche, publiés ou non, émanant des établissements d'enseignement et de recherche français ou étrangers, des laboratoires publics ou privés.

A compact dual-band dual-port diversity antenna for LTE

**Lila Mouffok^{*}, Anne Claire Lepage, Julien Sarrazin,
and Xavier Begaud**

Institut Telecom, Telecom ParisTech- LTCI CNRS UMR 5141 Paris, France

*corresponding author, E-mail: lila.mouffok@telecom-paristech.fr

Abstract

The design of a compact dual-band dual-port antenna system is presented. It operates in two frequency bands, 790-862 MHz and 2500-2690 MHz, thereby making it suitable for Long Term Evolution (LTE) handheld devices. The proposed system is composed of two orthogonal inverted-F antennas (IFA) to perform diversity in mobile terminals. A good agreement is observed between simulated and experimental results. The high antenna diversity capability of the proposed system is highlighted with the calculation of envelope correlation coefficient, mean effective and diversity gains for different environment scenarios.

1. Introduction

The use of multiple antennas can improve reliability and increase the channel capacity [1]. However, for wireless mobile devices, the available space is limited. Therefore, compact antenna systems are required. Recently, a variety of compact antennas for MIMO (Multiple-Input Multiple-Output) systems have been presented. An internal loop antenna with distributed feed which operates in LTE 700 MHz and GSM 800 MHz bands is presented in [2]. In this solution the two operating bandwidths are close. A dual port ferrite antenna is presented in [3] which operates in LTE 700 MHz but with low gain (-8 dBi). In [4], to achieve compactness, a PIFA is top loaded with a dielectric sheet. This solution covers the bands: 1710-1880 MHz, DCS 1800 MHz, and 2.5-2.69 GHz. Significant research has been made on dual-port and multiband antennas. However, there are few solutions covering two bands which are separated by more than an octave such as LTE bands (790-862 MHz and 2.5-2.69 GHz), with implementation of MIMO, for handheld devices.

Thus, the objective of the work presented in this paper is to propose a compact antenna system for mobile devices that operates in the above mentioned bands.

2. Antenna design

The proposed structure is printed on FR4 substrate with $\epsilon_r=3.7$, $\tan \delta=0.019$, and thickness of 0.7 mm (fig.1). The dimensions of the ground plane are $L \times L = 70 \times 70 \text{ mm}^2$ ($\lambda_0/5 \times \lambda_0/5$) where λ_0 is the free space wavelength of the lower band central frequency ($f_l=816 \text{ MHz}$). The structure is composed of two identical elements shaped IFA

(Inverted-F Antenna) located orthogonally to each other. The longer monopole allows operation on the lower band. It is connected to the ground plane with a metallic via hole to improve impedance matching. Its dimensions are $l_1=60 \text{ mm}$ ($\lambda_0/6$), and $h_1=16 \text{ mm}$ ($\lambda_0/22$). The shorter L shaped monopole controls the higher band operation with dimensions of $l_2=7.6 \text{ mm}$ ($\lambda_0/15$) and $h_2=8.4 \text{ mm}$ ($\lambda_0/13$) where λ_0 is the free space wavelength of the higher band central frequency ($f_2=2.6 \text{ GHz}$). The two monopoles are fed by two 50 Ohms SMA connectors (fig.1.b).

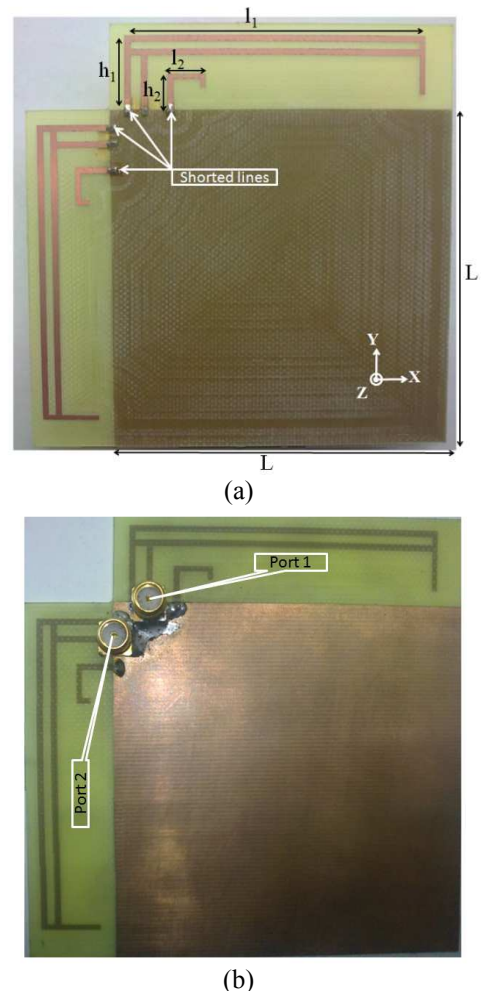


Figure 1: Photography and dimensions of the realized structure: (a) top view, (b) Bottom view.

3. Experimental results and discussions

The proposed structure has been simulated with the transient solver of CST Microwave Studio® and a prototype has been fabricated. Simulated and measured S-parameters are compared in Fig.2. A similar behavior between simulations and measurements is obtained. The structure operates in two bands ($|S_{11}| < -6$ dB): the lower band is about 10% (777-862 MHz) and the higher one about 8 % (2.49-2.70 GHz). The mutual coupling between the two ports is less than -6 dB in the lower band and -13 dB in the higher one.

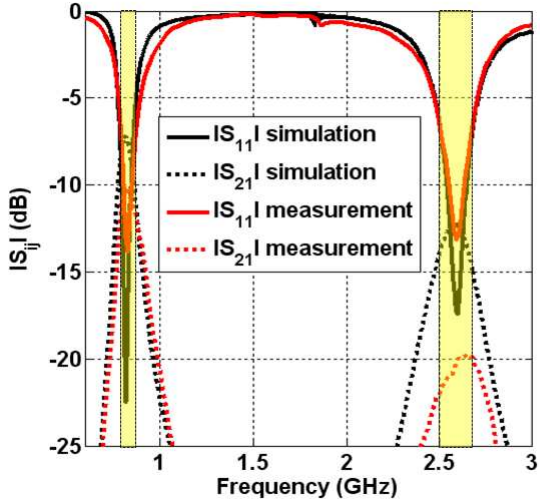
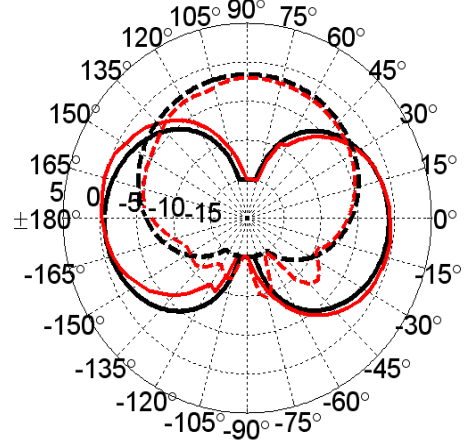


Figure 2: Simulated and measured S-parameters.

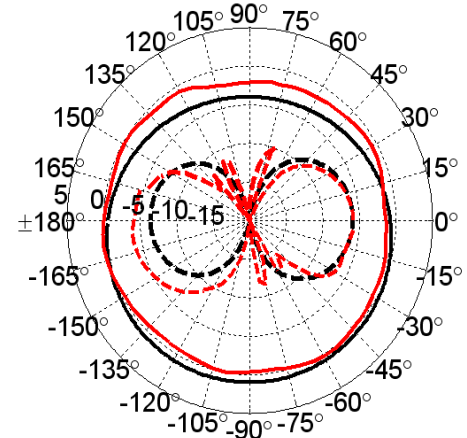
Fig.3 compares the simulated and measured co-polar and cross-polar radiation patterns in the E plane (YZ plane) and H plane (XZ plane) respectively. Because both ports are symmetrical, we only present radiation patterns for port 1 at 816 MHz and 2.6 GHz (port 2 being connected to a 50Ω). Polarization diversity is naturally achieved because of the orthogonal positions of both antennas. For both planes and both bands, it is found that the simulated and the measured radiation patterns are in good agreement.

In the lower band, the measured cross-polar level is about 10 dB lower than the co-polar level in the H plane but it increases in the E plane at 90° direction. This is due to the coupling with the second radiating element.

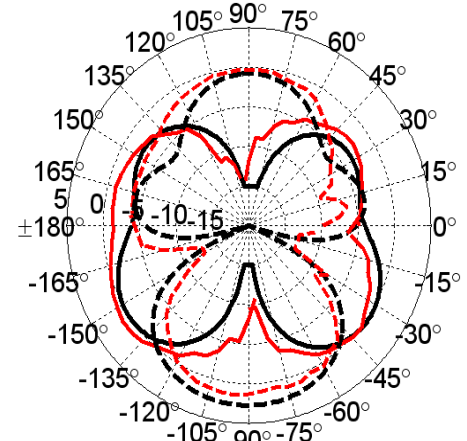
— Co-polar simulation
— Co-polar measurement
- - Cross-polar simulation
- - Cross-polar measurement



(a)



(b)



(c)

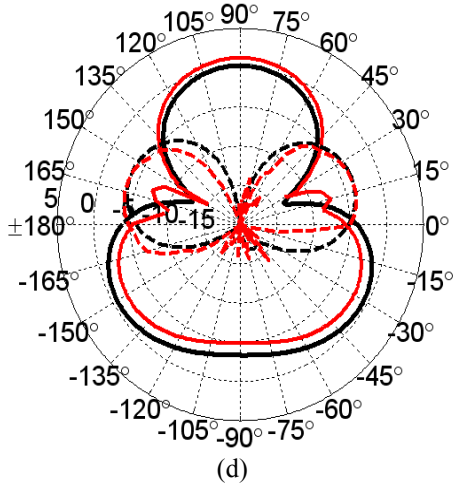


Figure 3: Simulated and measured radiation patterns: (a) in the E plane at 816 MHz, (b) in the H plane at 816 MHz, (c) in the E plane at 2.6 GHz, (d) in the H plane at 2.6 GHz.

To further investigate the diversity, the simulated radiation patterns of each antenna in the XY plane for the two bands are plotted in Fig.4 (one port is excited while the other one is loaded by 50 ohms). Thanks to a good agreement observed in Fig.3 between simulations and measurement, only simulations results are presented. As it can be observed for the lower band, quasi-orthogonality between the patterns is achieved. The maximum realized gain is about 1 dB at 0° for the port 1 and 1 dB at -90° for the port 2. The realized gain, by definition, takes into account the reflection coefficient at each port.

For the higher band, the maximum realized gain is 3.5 dB. At 2.6 GHz, even if patterns are not orthogonal, the two monopoles present minimum and maximum gain in different directions. This is well-suited to provide high diversity capabilities.

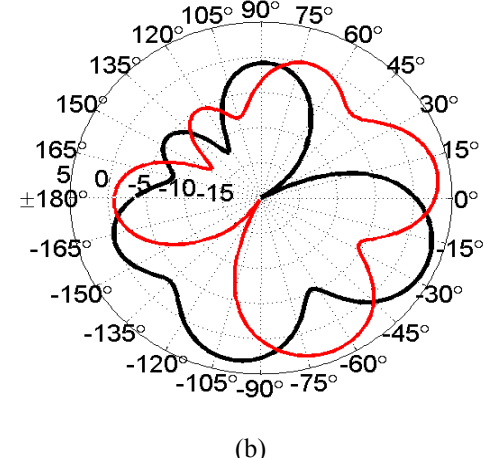
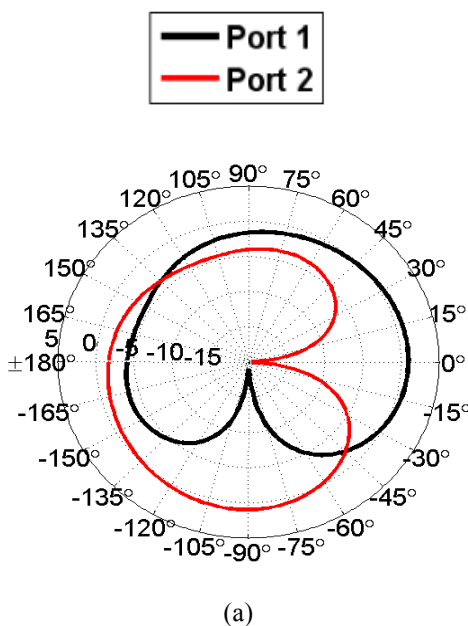


Figure 4: Realized total gain (dB) in the XY plane for the two bands: (a) at 816 MHz (b) at 2.6 GHz.

4. Evaluation of the diversity performance

In this section, we propose to evaluate the diversity performance of the proposed antenna by calculating the envelope correlation coefficient, the mean effective gain and the diversity gain while taking into account the propagation environment.

The envelope correlation coefficient ρ_e quantifies the similarity between the radiation patterns of the two monopoles. The lower the correlation, the better the diversity performance. Vaughan shows in [5] that this coefficient can be expressed by (1) using the complex electric field radiated by each antenna.

(1)

$$\rho_e = \frac{\left| \int_{\Omega} (E_{1\theta} E_{2\theta}^* p_\theta + XPD E_{1\varphi} E_{2\varphi}^* p_\varphi) d\Omega \right|^2}{\int_{\Omega} (E_{1\theta} E_{1\theta}^* p_\theta + XPD E_{1\varphi} E_{1\varphi}^* p_\varphi) d\Omega \int_{\Omega} (E_{2\theta} E_{2\theta}^* p_\theta + XPD E_{2\varphi} E_{2\varphi}^* p_\varphi) d\Omega}$$

$E_{1\theta}(\Omega), E_{1\varphi}(\Omega), E_{2\theta}(\Omega), E_{2\varphi}(\Omega)$ are complex electric fields along θ and φ radiated by the antenna fed by two different ports. The solid angle Ω is defined by θ [0: π] in elevation and φ [0: 2π] in azimuth. $p_\theta(\Omega)$ and $p_\varphi(\Omega)$ are the Angle-of-Arrival (AoA) distributions of incoming waves. The parameter XPD is the cross-polarization discrimination of the incident field and is defined as $XPD = S_\varphi/S_\theta$ (where S_φ and S_θ represent the average power along the spherical coordinates φ and θ). The environment depends strongly on the arrival angles distribution and on XPD. The most common distributions proven by measurements are Gaussian and Laplacian distributions [6]. Thus, we consider different distributions in elevation, while in azimuth plane the distribution will be uniform, as demonstrated by the two main measurement campaigns in the literature [6], [8]. In order to obtain more realistic results, different environments are considered. Each environment is characterized by typical values of XPD, mean angle of incident wave

distribution (θ_i) and standard deviation of wave distribution (σ). These values were deduced from several measurements [6], [7], [8] for different environments: isotropic, indoor, and outdoor. The isotropic environment is defined by XPD=0 dB, $p_\theta(\Omega)=p_\phi(\Omega)=1$, the indoor environment by XPD=1 dB, $\theta_i=20^\circ$, $\sigma=30^\circ$ and the outdoor environment by XPD=5 dB, $\theta_i=10^\circ$, $\sigma=15^\circ$.

The envelope correlation coefficient of the proposed structure has been calculated from simulated radiation patterns. Results are given in Fig.5.

For the lower band, the correlation coefficient is higher at extremities than at the center of the band, for all environments (see Fig. 5a). Note that correlation takes into account the radiation, matching and isolation level at each frequency. According to S-parameters levels, the correlation is more or less higher. Since IS_{111} variation over the whole band is more significant (from -6 dB to -20 dB) than IS_{211} variation (from -6 to -8 dB), ρ_e variation depends mainly on IS_{111} variation. Thus, the lower IS_{111} is, the lower ρ_e is.

For the higher band, the maximum value is below 0.08 which is less than in the lower band, thanks to a better isolation (<-13 dB). However, the ρ_e levels remain below 0.16 for the two bands which largely satisfies the condition ($\rho_e < 0.5$) to provide high diversity capabilities [5].

In the following part, we evaluate the Mean Effective Gain (MEG) which was introduced by Taga [9]. It is defined as the ratio between the mean received power of antennas over the random route and the total mean incident power. When each monopole receives the same quantity of power, the MEG ratio of the two monopoles is equal to one, which means that no performance deterioration is expected due to some power imbalance [10]. The mathematical expression is given by the equation (2):

$$MEG = \int_0^{2\pi} \int_0^{\pi} \left(\frac{XPD}{XPD+1} G_\theta p_\theta + \frac{1}{XPD+1} G_\phi p_\phi \right) d\Omega \quad (2)$$

Where G_θ and G_ϕ are the θ and ϕ components of the antenna power gain pattern respectively.

The calculated mean effective gains of the monopoles from simulated radiation patterns in the two bands are presented in Table I. It can be seen that the ratio of MEG_1 , determined at port 1, over MEG_2 , determined at port 2, is almost equal to 1, which satisfied equal contribution of the two monopoles to receive the same quantity of power. This is due to the fact that the proposed structure is completely symmetric and that the Gaussian and Laplacian angular distributions are taken only along the elevation as presented in [6].

Finally, the efficiency of the diversity is usually presented in terms of diversity gain (DG). It can be defined as the difference between the signal-to-noise ratio (SNR) of the combined signals and the SNR of a single antenna. In theory, the maximum gain estimated for diversity of two antennas is 10.2 dB [11]. It can be seen in Table 1 that calculated DG is about 10 dB across the whole desired bands, which is very satisfactory.

From the results shown in Fig.5 and Table 1, it is found that the received signals satisfy the conditions $\rho_e < 0.5$, $MEG_1/MEG_2 \approx 1$ and allows a diversity gain of 10 dB. These values fit the diversity requirements of MIMO systems.

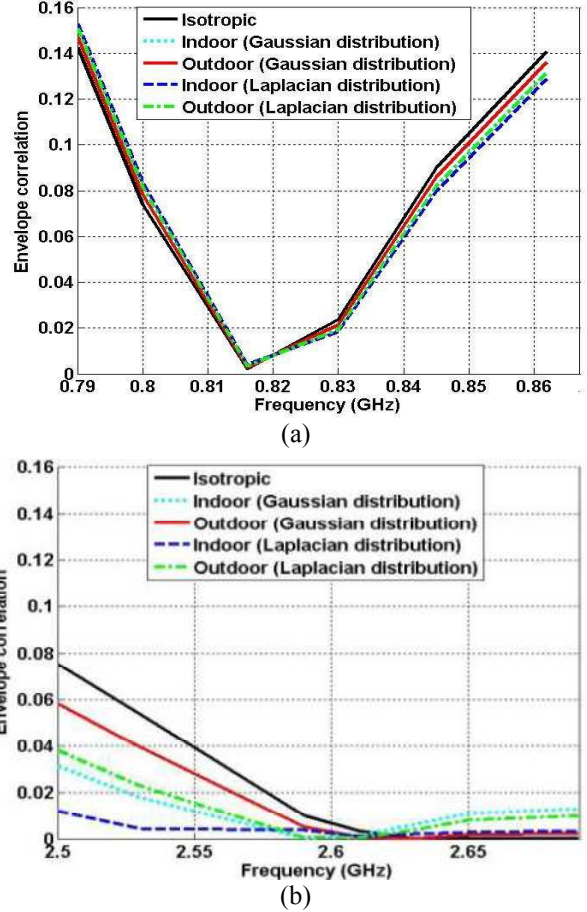


Figure 5: Envelope correlation for different environments of the proposed structure: (a) in the lower band (b) in the higher band.

Table 1: Diversity performances of the proposed antenna.

	MEG_1/MEG_2		Diversity gain (dB)	
	816 MHz	2.6 GHz	816 MHz	2.6 GHz
Isotropic	-4.33/-4.35	-4.93/-4.91	9.9	9.9
Indoor Gaussian	-5.03/-5.05	-5.17/-5.15	9.9	10
Outdoor Gaussian	-7.63/-7.64	-7.18/-7.15	9.9	9.9
Indoor Laplacian	-5.04/-5.05	-5.17/-5.15	9.9	10
Outdoor Laplacian	-7.63/-7.64	-7.18/-7.15	9.9	9.9

5. Conclusions

In this paper, a compact dual-band dual-port system for handheld devices has been proposed. The radiation element has an advantage to be only $60 \times 16 \text{ mm}^2 (\lambda_{01}/6 * \lambda_{01}/22)$, thus it can be easily implemented in mobile terminals. In addition, it covers two bands which are separated by more than an octave. The system provides good diversity capabilities thanks to a low correlation coefficient ($\rho_e < 0.2$), an equal amount of received power between the two radiating elements ($MEG_1/MEG_2 \approx 1$), and a diversity gain equal to 10 dB for different environments: isotropic, indoor and outdoor. Consequently, the presented design is suitable for MIMO communication applications.

Acknowledgements

The research leading to these results has received funding from the European Community's Seventh Framework Program (FP7/2007-2013) under grant agreement SACRA n° 249060.

References

- [1] G. S. Foschini, M. J. Gans, On limits of wireless communications in a fading environment when using multiple antennas, *Wireless Personal Communications*, Vol. 6, 311–335, 1998.
- [2] S. J. Eom, J. H. Lee, A. Kim, S. O. Park, Broadband internal antenna for 700 MHz LTE application with distributed feeders, *IEEE Microwave conference, APMC, Asia Pacific*, 1845–1848, 2009.
- [3] J. Lee, Y. K. Hong, S. Bae, G.S. Abo, W.M Seong, G. H. Kim, Miniature Long-Term Evolution (LTE) MIMO ferrite antenna, *IEEE Antennas Wireless Propag. Lett.*, Vol.10, 603–606, 2011.
- [4] A. N. Kulkarni, S. K. Sharma, A compact multiband antenna with MIMO implementation for USB Size 4G LTE wireless devices, *IEEE International Symposium on Antennas and Propag. (APSURSI)*, vol.10, 2215–2218, 2011.
- [5] R. J. Vaughan, J. B. Andersen, Antenna diversity in mobile communication, *IEEE Trans. on Vehicular Technology*, vol. 36, 149–172, 1987.
- [6] K. Kalliola, K. Sulonen, H. Laitinen, O. Kivekas, J. Krogerus, P. Vainikainen, Angular power distribution and mean effective gain of mobile antenna in different propagation environments, *IEEE Trans. on Vehicular Technology*, vol.51, 823– 838, 2002.
- [7] Z. Ying, T. Bolin, V. Plicanic, A. Derneryd, G. Kristensson, Diversity antenna terminal evaluation, *IEEE Antennas and Propagation Society International Symposium*, vol. 2A, 375– 378, 2005.
- [8] F. Adachi, M. Feeney, , J. Parsons, A. Williamson, Cross correlation between the envelopes of 900 MHz signals received at a mobile radio base station site, *Communications, Radar and Signal Processing, IEE Proceedings F*, vol. 133, 506-512, 1986.
- [9] T. Taga, Analysis for mean effective gain of mobile antennas in land mobile radio environments, *IEEE Trans. on Vehicular Technology*. vol. 39, 117-131, 1990.
- [10] T.W.C. Brown, Antenna diversity for mobile terminal, phD. Dissertation, Univ. Surrey, Surrey, U.K., 2002.
- [11] A. Diallo, C. Luxey, Estimation of the diversity performance of several two-antenna systems in different propagation environments, *Antennas and Propagation Society International Symposium*, 2642–2645, 2007.